



Temperature effect on vibrational properties of crystalline *p*-quaterphenyl[☆]

HPSTAR
714-2019

Kai Zhang^{a, b, c}, Xiao-Jia Chen^{c, *}

^aKey Laboratory of Materials Physics, Institute of Solid State Physics, Chinese Academy of Sciences, Hefei 230031, China

^bUniversity of Science and Technology of China, Hefei 230026, China

^cCenter for High Pressure Science and Technology Advanced Research, Shanghai 201203, China

ARTICLE INFO

Article history:

Received 13 November 2018

Received in revised form 23 December 2018

Accepted 13 January 2019

Available online 16 January 2019

Keywords:

p-Quaterphenyl

Raman spectroscopy

Vibrational properties

Low temperature

ABSTRACT

Vibrational properties of the crystalline *p*-quaterphenyl at low temperature are investigated by Raman scattering. The temperature dependent vibrational behaviors associated with the intra- and intermolecular terms are analyzed in detail. The order-disorder transition makes significant impacts on the energies, widths, and intensities of the vibrational modes, and the drastic splits of the modes mainly result from the sudden decline of the peak widths. Meanwhile, the intensity ratio of the 1280-cm⁻¹ and 1220-cm⁻¹ mode exhibits anomalous tendency around the transition temperature, as well as the frequency separations between them and between the higher energy mode and the lower energy mode around 1600 cm⁻¹. Thus, they still can well indicate the molecular planarity in the low temperature conditions. However, the intensity ratio of the two modes around 1600 cm⁻¹ is no longer to be a good indicator of this transition due to the bare anomalous behavior around the transition temperature. Our work is of important significance for understanding the internal vibrational properties of *p*-quaterphenyl, and it also provides considerable supports for the further study of this material.

© 2019 Elsevier B.V. All rights reserved.

1. Introduction

Seeking novel properties in organic materials, such as the better electronic conductivity, thermoelectricity, and even superconductivity, is always an interesting and significant study for the scientific research and applications. Among the organics, poly(*para*-phenylene) (PPP) have received a lot of attentions as the excellent performance which is resulted from the typical structure. Those materials all have the structure with phenyl rings connecting at the *para* positions. This typical structure generates large delocalized π -electrons along the molecular chain, and it contributes to improve the electron-transporting properties. The oligomeric lower members of PPP are always named with the prexes (ter-, quater-, quinque-, sexi-, septi-, etc.), which signify the phenyl numbers in one molecule, placed in front of the radical name phenyl. *p*-Oligophenylys always exhibit insulating or semiconducting behaviors in their normal state, whereas they have several orders increase of magnitude on the conductivity after electron donors or acceptors doping [1–6]. Moreover, superconductivity has been recently discovered in the alkalis-metal

doped *p*-oligophenylys and their derivatives [7–14]. Multiple superconducting phases with the transition temperatures of 4 K, 7 K, and even 120 K, which is comparable with most cuprate superconductors [15], form after doping. This finding implies that the organic materials have tremendous potential to be high temperature even room temperature superconductors. PPP materials also possess potential thermoelectric applications due to the drastic increase of the conductivity [16–18]. On the other hand, this typical structure makes the neighboring phenyl rings strongly librate around the long molecular axis which is resulted from the competition between two contrary types of forces of the steric repulsion between the neighboring four H atoms and the conjugation resulting from the delocalized π -electrons [19,20]. However, the phenyl rings in the individual molecules are confirmed parallel to each other on average even though the thermal librations are strong in the crystals [21–25]. Interestingly, the molecules become non-planar arising from the freeze of the molecular librations at low temperature, *i.e.*, angles with stable values appear between the neighboring rings [21–25]. Moreover, the torsion angles of the adjacent molecules along the *a* and *b* crystal axes are further confirmed opposite with each other. Thus, the lattice parameters *a* and *b* will have double enlargements. Such a structural transition can have significant impacts on the natural properties of *p*-oligophenylys [25–32]. Since the 120-K superconducting phase was found in the potassium-doped *p*-quaterphenyl, studies of the properties of it become increasingly interesting and requisite.

p-Quaterphenyl exhibits semiconducting behavior at normal state. This material and its derivatives are always extensively applied

[☆] Fully documented templates are available in the elsarticle package on CTAN.

* Corresponding author.

E-mail address: xjchen@hpstar.ac.cn (X.-J. Chen).

in organic thin film transistors [33], organic light emitting diodes [34], and organic lasers [35,36] due to the excellent optical activation [37]. *p*-Quaterphenyl exhibits a monoclinic structure at ambient condition, and it is confirmed to occur an “order-disorder” type structural transition at 233 K [31]. This transition shares the same behaviors with *p*-terphenyl [38,39]. Raman spectroscopy is a powerful method to detect this transition. A plenty of works have been performed on biphenyl and *p*-terphenyl. However, to data, only a few works have been taken to study the vibrational properties of the low frequency phonon bands of *p*-quaterphenyl [40], study of the high energy band behaviors is rare. Thus, comprehensive analyses of the vibrational properties of *p*-quaterphenyl are essential for the further study.

In this work, we measure the 660-nm laser excited Raman spectra of *p*-quaterphenyl from 5 K to 350 K. The vibrational properties of the phonon bands from the lattice vibrations to the high frequency modes of C—H vibrations are comprehensively analyzed and compared to biphenyl and *p*-terphenyl to study the order-disorder phase transition occurred at around 233 K. Our work provides a basic footstone for the further study of *p*-quaterphenyl.

2. Experimental Details

In the experiment the high-purity *p*-quaterphenyl was purchased from Alfa Aesarare. The sample was sealed in quartz tubes with the diameter of 1 mm for Raman-scattering experiment in a glove box with the moisture and oxygen levels less than 0.1 ppm. The wavelength of the exciting laser beam was 660 nm. The power was less than 1 mW before a $\times 20$ objective to avoid possible damage of sample. An integration time of 20 s was used to obtain the spectra. The scattered light was focused on 1200 g/mm grating and then recorded with a 1024 pixel Charge Coupled Device designed by Princeton.

3. Results and Discussion

We measured the Raman spectra of *p*-quaterphenyl at the temperature range from 5 K to 350 K by a 660-nm excitation. All the spectra have obvious broad fluorescent background, and they seemingly exhibit a growing tendency with decreasing temperature. In order to analyze the vibration modes, a constant background was removed from the raw data. Then the scattering intensity was normalized by the statistical factor n for the Stokes side by

$$I(\omega) = I_0(\omega) / [n(\omega, T) + 1] \quad (1)$$

where $n(\omega, T)$ is the Bose-Einstein distribution function evaluated at mode energy ω and temperature T , and $I_0(\omega)$ is the observed intensity. The scattering intensity is very sensitive to the temperature because that the intensity of the low frequency modes increases with decreasing temperature whereas it decreases before normalizing. The normalized Raman spectra at 300 K, 200 K, 100 K, and 5 K are presented in Fig. 1. The Raman spectra of *p*-quaterphenyl show more complex behaviors than *p*-terphenyl. Such a situation should result from the additional phenyl ring and the different symmetry compared with *p*-terphenyl. In the whole temperature range, no additional peaks can be observed. This indicates that this transition belongs to order-disorder transition which has not any structural modulation. In addition, nearly all the vibrational modes increase their intensities as temperature is decreased, and their full widths at half maximum (FWHMs) simultaneously decrease. That is also the reason why the phonon bands, especially the librational motion modes, exhibit obvious splits at low temperature. A broad peak appears at low temperatures, which can also be seen in biphenyl and *p*-terphenyl [42]. This peak should result from the fluorescence effects.

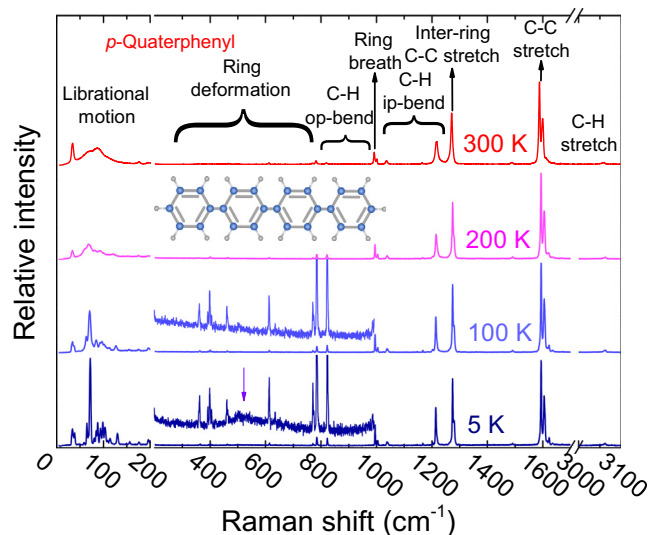


Fig. 1. 660-nm laser excited Raman spectra of *p*-quaterphenyl at 300 K, 200 K, 100 K, and 5 K. The spectra have displaced vertically for clarity. All the spectra are broken between 1700 cm^{-1} and 3000 cm^{-1} which no phonon bands are observed. Classifications of the vibration modes over the spectrum of 300 K were taken from Ref. [41],[41]

Detailed evolution of the low frequency modes is presented in Fig. 2 (a). Modes in this energy range are corresponding to the lattice vibrations. The upper figure in Fig. 2 (a) is the temperature evolutionary Raman intensity maps of *p*-quaterphenyl, and the bottom depicts the Raman spectra at 5 K and 350 K and the details of the fitting results for clarify. Upon cooling, the scattering intensities of all the modes increase. And below around the transition temperature of 233 K [31], the librational peaks all exhibit dramatic splits. At 5 K, at least 18 peaks appear in the frequency range from 5 to 170 cm^{-1} . In those peaks, the lowest energy peak always draws a lot of attention due to the anomalous tendency on the FWHM, which is confirmed resulting from the anharmonic effect. This characteristic behavior makes this peak a good indicator of the order-disorder transition [30,42,43]. We fitted the lowest energy peak with the Lorentzian function. Details of the fitting models are shown in Fig. 2 (a), and the fitted frequencies and FWHMs are shown in Fig. 2 (b). The energy of this peak rapidly increases with decreasing temperature. Below the transition temperature, the increase rate decreases. Meanwhile, its FWHM exhibits a sudden drop from an almost constant value at this temperature. It indicates that the anharmonic effect of the phonons drastic decreases after entering into the ordered state. Other modes also have the same modifications. This is the dominating reason to result in the peak splits after the transition temperature. It is worth mentioning that the anomalous temperature in our experiment is about 240 K. It is a little higher than 233 K confirmed by specific heat measurements, such a case should arise from the thermal fluctuations [31,42].

The two modes at around 1220 cm^{-1} and 1280 cm^{-1} are always used to as the molecular chain length and planarity indicators in PPP materials [44–49]. The detailed temperature evolutionary spectra of *p*-quaterphenyl in the frequency range from 1170 cm^{-1} to 1320 cm^{-1} are painted in Fig. 3 (a). In this figure, these two peaks all show anomalous changes not only on the frequencies but also on the FWHMs and intensities with decreasing temperature. Below the transition temperature, all these two modes have drastic splits. In addition, one can also see that the 1220- cm^{-1} mode shows more complicated behaviors than 1280 cm^{-1} mode. In order to analyze the properties of these two peaks, we fit them by Lorentzian function, results are shown in Fig. 3 (b) and (c). The frequency and

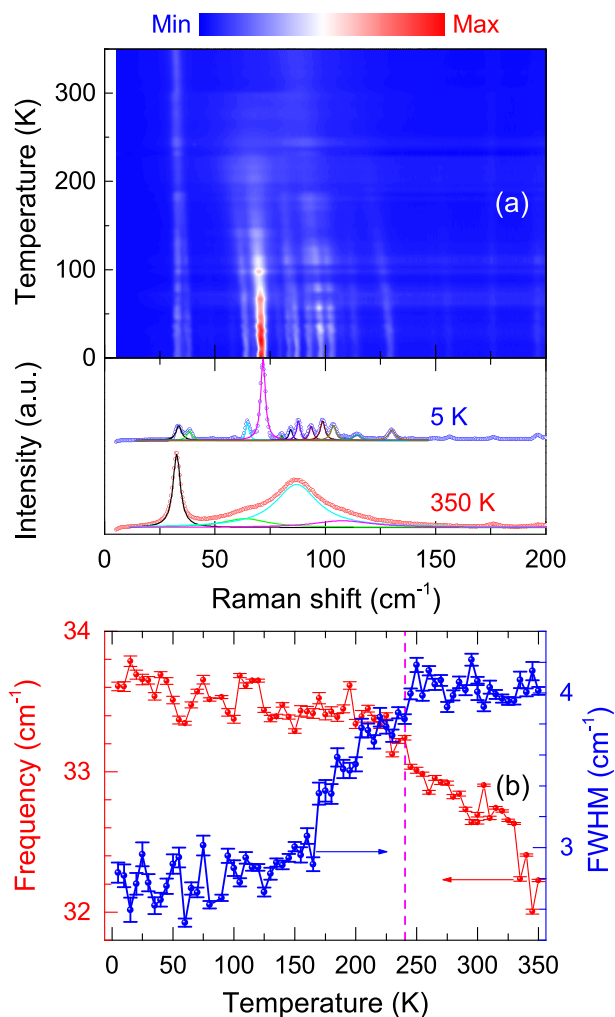


Fig. 2. (a) Raman spectra map of the low energy modes of *p*-terphenyl. The spectra at 350 K and 5 K are shown for clarity. (b) Frequency and FWHM of the lowest energy mode as a function of temperature. The vertical dashed line indicates the structural transition temperature of around 233 K.

FWHM of the 1220-cm⁻¹ mode almost have the same tendencies. They all first decrease as the temperature is decreased. After entering into the ordered state, their decline rate suddenly increases, and

then gradually decreases upon further cooling. The frequency of the 1280-cm⁻¹ mode firstly increases with decreasing the temperature, and then becomes constant after transition. The FWHM of this mode shares the same behavior with the 1220-cm⁻¹ mode. Such behaviors of these two modes are almost the same with *p*-terphenyl except the frequency tendency of the 1220-cm⁻¹ mode [42]. Previous works [47] proposed that the 1220-cm⁻¹ mode is closely related to the delocalized π -electrons stemmed from the C atoms on the long molecular axis, and the localized electrons of the off-axis C atoms make important contributions to 1280 cm⁻¹ mode. Thus, the former is susceptible to the conjugation effects, whereas the latter is far less. Our Raman data is well in accord with this scenario, the variations of the frequency, FWHM, and even the intensity of the former mode is visibly greater than the latter mode (see in Fig. 3 (a)). On the other hand, the anomalous frequency behavior of the 1220-cm⁻¹ mode should result from the gradually increased angles among the phenyl rings in one molecule. With decreasing the temperature, the torsion angle between the neighboring phenyl rings increases. It will strongly impact the delocalized electrons, and the localized orbitals will be enhanced.

Fig. 3 (d) and (e) present the temperature dependent intensity ratio and frequency difference of the 1220-cm⁻¹ and 1280-cm⁻¹ modes, respectively. The intensity ratio of these two modes is always used to distinguish the phenyl ring numbers in PPP materials [44,48], and the frequency difference of them is also a good indicator of the molecular planarity [45–47, 49]. Upon cooling, an extreme point can be observed in the intensity ratio figure at around the order–disorder transition temperature. Meanwhile, the frequency difference also exhibits an inflexion point at the same temperature. These situations imply that these two indicators are also suitable for the low temperature case.

The two modes at around 1600 cm⁻¹ also possess interesting properties and thus are always used to estimate the planarity [44,48,50]. The Raman intensity map at around 1600 cm⁻¹ from 5 K to 350 K is painted in Fig. 4 (a), and the Raman spectra at 5 K and 350 K are provided in the bottom for clarity, as well as the fitting models. There are at least 6 peaks existed here. We fitted the two strong peaks (lower energy peak A and higher energy peak B), and the results are shown in Fig. 4 (b), (c), and (d). The frequencies of these two modes all increase with decreasing temperature, and the FWHMs of them simultaneously decrease. No special anomalies can be found in the frequency and FWHM tendencies except an inflexion point in the frequency data of the high energy peak. It almost shares the same behaviors with *p*-terphenyl [42]. We also calculated the intensity ratio I_B/I_A and the frequency difference $\omega_B - \omega_A$ of these two peaks. Their intensity ratio decreases as the temperature

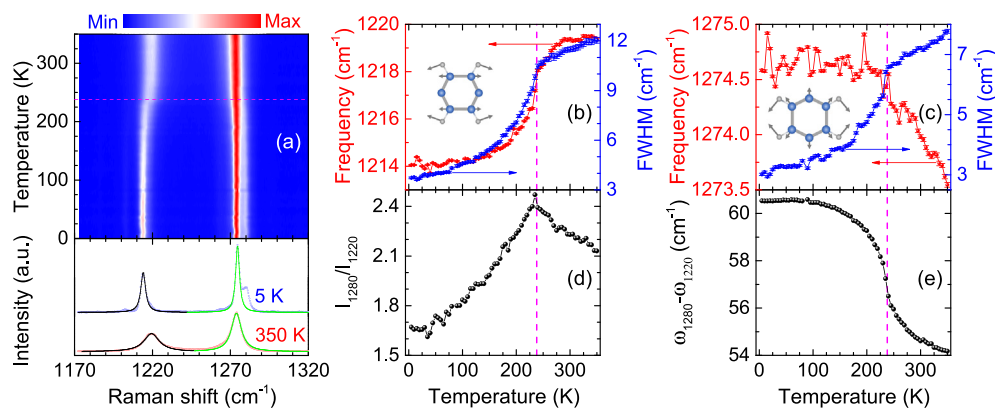


Fig. 3. (a) Raman spectra map of *p*-terphenyl at the frequencies around 1220 cm⁻¹ and 1280 cm⁻¹. Spectra at 350 K and 5 K are shown for clarity. (b) and (c) Frequencies and FWHMs of the 1220-cm⁻¹ mode and the 1280-cm⁻¹ mode as functions of temperature. (d) and (e) Temperature-dependent intensity ratio and frequency difference of these two modes. The vertical dashed lines indicate the structural transition temperature of around 233 K.

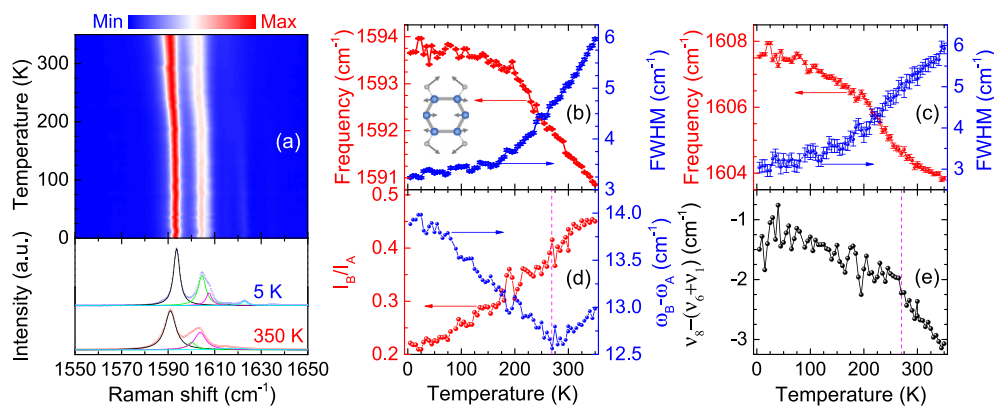


Fig. 4. (a) Raman spectra map of *p*-quaterphenyl at the frequencies around 1600 cm⁻¹. Spectra at 350 K and 5 K are shown for clarity. (b) and (c) Frequencies and FWHMs of the two modes at around 1600 cm⁻¹ as functions of temperature. (d) Temperature dependent intensity ratio of these two modes. (e) Temperature-dependent frequency difference and the difference between $\nu_6 + \nu_1$ and ν_8 . The vertical dashed lines indicate the structural transition temperature of around 233 K.

is decreased, and no any clear anomalies can be observed here. This indicates that the intensity ratio of these two modes is no longer a good indicator of the molecular conjugations at low temperature. The frequency difference of them exhibits a reverse tendency at around 270 K. This phenomenon should also result from the order-disorder transition, and this also signals that *p*-quaterphenyl already enters into the thermal anomalous state at around 270 K. Fig. 4 (e) is the energy separation between the higher energy peak and sum of the mode at 612 cm⁻¹ and the ring breathing mode at around 993 cm⁻¹. Previous works discovered that the higher energy peak is a combination mode of the latter two fundamental modes, and their energy difference is an indicator of the mode mixing level [48,50–53]. The gradually reduction of the separation with decreasing temperature indicates that the mixing level declines.

4. Conclusions

In conclusion, vibrational properties of the crystalline *p*-quaterphenyl have been investigated by Raman scattering with a 660-nm laser from 5 K to 350 K. Detailed analyses have been performed on the intra- and intermolecular terms to understand the phonon behaviors, and the results have been compared with biphenyl and *p*-terphenyl. The order-disorder transition temperature was confirmed at around 233 K, whereas most vibrational modes already show anomalous behaviors above this temperature due to the thermal fluctuations. Nearly all the modes were found to exist anomalous tendencies on the energies, widths, and intensities before and after the transition temperature, especially the phonon widths, it is the major reason to result in the peak splits at low temperatures. The intensity ratio of the 1280-cm⁻¹ mode and the 1220-cm⁻¹ mode is still a good indicator of the molecular planarity for *p*-quaterphenyl at low temperature, as well as the frequency separations between them and between the higher energy mode and the lower energy mode around 1600 cm⁻¹. However, the intensity ratio of the two modes at around 1600 cm⁻¹ has almost no obvious anomalies around the transition temperature, thus it can hardly indicate the molecular conjugation at low temperature. Our work provides the basis to understand the internal vibrational properties of *p*-quaterphenyl.

Acknowledgments

This work was supported by the National Key R&D Program of China (Grant No. 2018YFA0305900).

References

- [1] E.E. Havinga, L.W.V. Horsen, Dependence of the electrical conductivity of heavily-doped poly-*p*-phenylenes on the chain length, *Synth. Met.* 16 (1) (1986) 55–70.
- [2] D.M. Ivory, G.G. Miller, J.M. Sowa, L.W. Shacklette, R.R. Chance, R.H. Baughman, Highly conducting charge-transfer complexes of poly(*p*-phenylene), *J. Chem. Phys.* 71 (3) (1979) 1506–1507.
- [3] L.W. Shacklette, H. Eckhardt, R.R. Chance, G.G. Miller, D.M. Ivory, R.H. Baughman, Solidstate synthesis of highly conducting polyphenylene from crystalline oligomers, *J. Chem. Phys.* 73 (8) (1980) 4098–4102.
- [4] T. Minakata, M. Ozaki, H. Imai, Conducting thin films of pentacene doped with alkaline metals, *J. Appl. Phys.* 74 (2) (1993) 1079–1082.
- [5] Y. Matsuo, S. Sasaki, S. Ikehata, Stage structure and electrical properties of rubidium-doped pentacene, *Phys. Lett. A* 321 (1) (2004) 62–66.
- [6] Y. Kaneko, T. Suzuki, Y. Matsuo, S. Ikehata, Metallic electrical conduction in alkaline metal-doped pentacene, *Synth. Met.* 154 (1) (2005) 177–180.
- [7] G.H. Zhong, D.Y. Yang, K. Zhang, R.S. Wang, C. Zhang, H.Q. Lin, X.J. Chen, Superconductivity and phase stability of potassium-doped biphenyl, *Phys. Chem. Chem. Phys.* 20 (2018) 25217–25223.
- [8] R.S. Wang, J. Cheng, X.L. Wu, H. Yang, X.J. Chen, Y. Gao, Z.B. Huang, Superconductivity at 3.5 K and/or 7.2 K in potassium-doped triphenylbismuth, *J. Chem. Phys.* 149 (2018) 144502.
- [9] R.S. Wang, Y. Gao, Z.B. Huang, X.J. Chen, Superconductivity in *p*-Terphenyl, arXiv:1703.05803, 2017.
- [10] R.S. Wang, Y. Gao, Z.B. Huang, X.J. Chen, Superconductivity at 43 K in a Single C—C Bond Linked Terphenyl, arXiv:1703.05804, 2017.
- [11] R.S. Wang, Y. Gao, Z.B. Huang, X.J. Chen, Superconductivity Above 120 Kelvin in a Chain Link Molecule, arXiv:1703.06641, 2017.
- [12] J.F. Yan, G.H. Zhong, R.S. Wang, K. Zhang, H.Q. Lin, X.J. Chen, Superconductivity and phase stability of potassium-intercalated *p*-quaterphenyl, *J. Phys. Chem. Lett.* 10 (2019) 40–47. <https://doi.org/10.1021/acs.jpcclett.8b03263>.
- [13] G. Huang, G.H. Zhong, R.S. Wang, J.X. Han, H.Q. Lin, X.J. Chen, Superconductivity and phase stability of potassium-doped *p*-quinquephenyl, *Carbon* 143 (2019) 837–843.
- [14] M.V. Mazziotti, A. Valletta, G. Campi, D. Innocenti, A. Perali, A. Bianconi, Possible Fano resonance for high T_c multi-gap superconductivity in *p*-terphenyl doped by K at the Lifshitz transition, *EPL (Europhysics Letters)* 118 (3) (2017) 37003.
- [15] S.N. Putilin, E.V. Antipov, M. Marezio, Superconductivity above 120 K in HgBa₂CaCu₂O_{6+δ}, *Physica C* 212 (34) (1993) 266–270.
- [16] N. Dubey, M. Leclerc, Conducting polymers: efficient thermoelectric materials, *J. Polym. Sci.* 49 (7) (2011) 467–475.
- [17] Y. Xuan, X. Liu, S. Desbief, P. Leclère, M. Fahlman, R. Lazzaroni, M. Berggren, J. Cornil, D. Emin, X. Crispin, Thermoelectric properties of conducting polymers: the case of poly(3-hexylthiophene), *Phys. Rev. B* 82 (11) (2010) 115454.
- [18] O. Bubnova, Z.U. Khan, A. Malti, S. Braun, M. Fahlman, M. Berggren, X. Crispin, Optimization of the thermoelectric figure of merit in the conducting polymer poly(3,4-ethylenedioxythiophene), *Nat. Mater.* 10 (6) (2011) 429–433.
- [19] L.A. Carreira, T.G. Towns, Raman spectra and barriers to internal rotation: biphenyl and nitrobenzene, *J. Mol. Struct.* 41 (52) (1977) 1–9.
- [20] J. Soto, V. Hernández, J.T.L. Navarrete, Conformational study and lattice dynamics of poly(*p*-phenylene: oligomers and polymer), *Synth. Met.* 51 (51) (1992) 229–238.
- [21] G.P. Charbonneau, Y. Delugeard, Biphenyl: three-dimensional data and new refinement at 293 K, *Acta Crystallogr.* 33 (5) (1977) 1586–1588.
- [22] J.L. Baudour, H. Cailleau, W.B. Yelon, Structural phase transition in polyphenyls. IV. Double-well potential in the disordered phase of *p*-terphenyl from neutron (200 K) and X-ray (room-temperature) diffraction data, *Acta Crystallogr.* 33 (6) (1977) 1773–1780.

- [23] J.L. Baudour, Y. Delugeard, P. Rivet, Structural phase transition in polyphenyls. IV. Crystal structure of the low-temperature ordered phase of *p*-quaterphenyl at 110 K, *Acta Crystallogr.* 34 (2) (1978) 625–628.
- [24] Y. Delugeard, J. Desuche, J.L. Baudour, Structural transition in polyphenyls. II. The crystal structure of the high-temperature phase of quaterphenyl, *Acta Crystallogr.* 32 (3) (1976) 702–705.
- [25] L. Barba, G. Chita, G. Campi, L. Suber, E.M. Bauer, A. Marcelli, A. Bianconi, Anisotropic thermal expansion of *p*-terphenyl: a self-assembled supramolecular array of poly-*p*-phenyl nanoribbons, *J. Supercond. Nov. Magn.* 31 (3) (2018) 703–710.
- [26] P.S. Friedman, R. Kopelman, P.N. Prasad, Spectroscopic evidence for a continuous change in molecular and crystal structure: deformation of biphenyl in the low temperature solid, *Chem. Phys. Lett.* 24 (1) (1974) 15–17.
- [27] A. Bree, M. Edelson, A study of the second order phase transition in biphenyl at 40 K through Raman spectroscopy, *Chem. Phys. Lett.* 46 (3) (1977) 500–504.
- [28] T. Atake, H. Chihara, Heat capacity anomalies due to successive phase transitions in 1,1'-biphenyl, *Solid State Communications* 35 (2) (1980) 131–134.
- [29] S. Chang, Heat capacity and thermodynamic properties of *p*terphenyl: study of order-disorder transition by automated highresolution adiabatic calorimetry, *J. Chem. Phys.* 79 (12) (1983) 6229–6236.
- [30] A. Girard, H. Cailleau, Y. Marqueton, C. Ecolivet, Raman scattering study of the order-disorder phase transition in *para*-terphenyl, *Chem. Phys. Lett.* 54 (3) (1978) 479–482.
- [31] K. Saito, T. Atake, H. Chihara, Molar heat capacity and thermodynamic properties of *p*-quaterphenyl, *J. Chem. Thermodyn.* 17 (6) (1985) 539–548.
- [32] K. Saito, Y. Yamamura, M. Sorai, Twist phase transition in poly(*p*-phenylene) oligomers: heat capacity of *p*-quinquephenyl, *Bull. Chem. Soc. Jpn.* 73 (12) (2000) 2713–2718.
- [33] D.J. Gundlach, Y.Y. Lin, T.N. Jackson, D.G. Schlom, Oligophenyl-based organic thin film transistors, *Appl. Phys. Lett.* 71 (26) (1997) 3853–3855.
- [34] C. Hosokawa, H. Higashi, T. Kusumoto, Novel structure of organic electroluminescence cells with conjugated oligomers, *Appl. Phys. Lett.* 62 (25) (1993) 3238–3240.
- [35] F. Quochi, Random lasers based on organic epitaxial nanofibers, *J. Opt.* 12 (2) (2010) 024003.
- [36] J. Lu, K. Miyatake, A.R. Hlil, A.S. Hay, Novel soluble and fluorescent poly(arylene ether)s containing *p*-quaterphenyl, 2,5-bis(4-phenylphenyl)oxadiazole, or 2,5-bis(4-phenylphenyl)triazole groups, *Macromolecules* 34 (17) (2001) 5860–5867.
- [37] G. Leising, S. Tasch, F. Meghdadi, L. Athouel, G. Froyer, U. Scherf, Blue electroluminescence with ladder-type poly(*para*-phenylene) and *para*-hexaphenyl, *Synth. Met.* 81 (23) (1996) 185–189.
- [38] J.L. Baudour, Y. Delugeard, H. Cailleau, Transition structurale dans les polyphényles. I. Structure cristalline de la phase basse température du *p*-terphényle à 113 K, *Acta Crystallogr. B* 32 (1) (1976) 150–154.
- [39] P. Bordat, R. Brown, A molecular model of *p*-terphenyl and its disorder-order transition, *Chem. Phys.* 246 (1-3) (1999) 323–334.
- [40] B.A. Bolton, P.N. Prasad, Phase transitions in polyphenyls: Raman spectra of *p*-terphenyl and *p*-quaterphenyl in the solid state, *Chem. Phys.* 35 (3) (1978) 331–344.
- [41] K. Honda, Y. Furukawa, Conformational analysis of *p*-terphenyl by vibrational spectroscopy and density functional theory calculations, *J. Mol. Struct.* 735–736 (2005) 11–19.
- [42] K. Zhang, R.-S. Wang, X.-J. Chen, Vibrational properties of *p*-terphenyl, *J. Phys. Chem. A* 122 (34) (2018) 6903–6908.
- [43] A. Girard, M. Sanquer, Y. Dëlugeard, Low-frequency Raman study of *para*-terphenyl: influence of the isotopic substitution and interpretation of the spectra in both phases, *Chem. Phys.* 96 (3) (1985) 427–434.
- [44] H. Ohtsuka, Y. Furukawa, M. Tasumi, Dependencies of the Raman spectra of *p*-oligophenyls on the chain length and the excitation wavelength, *Spectrochim. Acta* 49 (5-6) (1993) 731–737.
- [45] G. Heimel, D. Somitsch, P. Knoll, E. Zojer, Albrecht theory and anharmonic coupling in polyphenyl Raman spectra, *Synth. Met.* 139 (3) (2003) 823–825.
- [46] L. Cuff, M. Kertesz, *Ab initio* oligomer approach to vibrational spectra of polymers: comparison of helical and planar poly(*p*-phenylene), *Macromolecules* 27 (3) (1994) 762–770.
- [47] G. Heimel, D. Somitsch, P. Knoll, J.L. Brédas, E. Zojer, Effective conjugation and Raman intensities in oligo(*para*-phenylene)s: a microscopic view from first-principles calculations, *J. Chem. Phys.* 122 (11) (2005) 114511.
- [48] K. Zhang, X.J. Chen, Chain length effects of *p*-oligophenyls with comparison of benzene by Raman scattering, *AIP Adv.* 8 (2) (2018) 025004.
- [49] Identification of the incommensurate structure transition in biphenyl by Raman scattering, *Spectrochim. Acta* 206 (2019) 202–206.
- [50] G. Heimel, D. Somitsch, P. Knoll, E. Zojer, *Ab initio* study of vibrational anharmonic coupling effects in oligo(*para*-phenylenes), *J. Chem. Phys.* 116 (24) (2002) 10921–10931.
- [51] E.B. Wilson, Jr, The normal modes and frequencies of vibration of the regular plane hexagon model of the benzene molecule, *Phys. Rev.* 45 (10) (1934) 706–714.
- [52] W.R. Angus, C.R. Bailey, J.B. Hale, C.K. Ingold, A.H. Leckie, C.G. Raisin, J.W. Thompson, C.L. Wilson, Structure of benzene. Part VIII. Assignment of vibration frequencies of benzene and hexadeuterobenzene, *J. Chem. Soc.* 218 (1936) 971–987.
- [53] M. Ito, T. Shigeoka, Raman spectra of benzene and benzene- d_6 crystals, *Spectrochim. Acta* 22 (6) (1966) 1029–1044.